Voltage-Base Control of Camera Stabilizer Using Optimal Adaptive Fuzzy Sliding Mode Control

Mohammad Veysi [1] **Mohammad Reza Soltanpour** [2]

[1] MSc, Department of Electrical Engineering, Khatam ol Anbia University, Tehran, Iran.
mohammad.veysi61@yahoo.com
[2] Associate Professor, Department of Electrical Engineering, Shahid Sattari Aeronautical University of Science and Technology, Tehran, Iran.
m_r_soltanpour@yahoo.com

Abstract:

The camera stabilizer stabilizes the camera's line of sight by isolating the camera from the model uncertainties, disturbances of operating environment and system movements. This paper presents a voltage-base optimal adaptive fuzzy sliding mode control for camera stabilizer. In this proposed control method, a voltage-base sliding mode controller is applied. But unfortunately, undesirable control input chattering is caused by employing the sliding mode control. In the following, for the prevention of incidence of the control input chattering, a first order TSK fuzzy approximator is employed. Although fuzzy sliding mode control prevents the chattering phenomenon, it has some disadvantages such as disability in estimating the bounds of the existing uncertainties and lack of stability proof of the closed-loop system. In what follows, to overcome the aforementioned problems, an adaptive fuzzy system is designed such that it can estimate the bounds of the existing uncertainties. Ultimately, the chicken swarm optimization algorithm is utilized to determine the optimal values of coefficients of the adaptive fuzzy sliding mode control and to decrease the control input amplitude. To investigate the desirable performance of the optimal adaptive fuzzy sliding mode controller, simulations in four steps are implemented on a camera stabilizer.

Keywords: Camera stabilizer; Voltage-base control; Optimal adaptive fuzzy sliding mode control; Uncertainty; Chattering; Inverse dynamic method.

Submission date: 13, April, 2016

Conditional acceptance date: 8, June, 2016

Acceptance date: 24, Sep., 2016

Corresponding author: MR. Soltanpour

Corresponding author's address: Department of Electrical Engineering, Shahid Sattari Aeronautical University of Science and Technology, Shamshiri Street, Tehran 1384673411, Iran.

[Downloaded from jiaeee.com on 2026-09-13]

[DOR: 20.1001.1.26765810.1396.14.4.3.0]

1. Introduction

The electro-optical sensing equipment such as camera systems are widely used in surveillance, monitoring, searching and scan operations and target tracking operations [1, 2]. Camera systems that are mounted on various systems such as missiles, aircrafts, UAVs, radars, boats and navigation instruments are subjected to vibrations introduced by system movements, base angular motion, the dynamics of camera system and the camera mass unbalance. These vibrations cause the line-of-sight (LOS) of the camera to shift, resulting in serious degradation of the image or video quality. So, a camera stabilizer is required to stabilize the LOS of camera against system movements and disturbances [3, 4].

The camera stabilizer has two gimbal axes, namely, yaw (azimuth) and pitch (elevation). The gimbal axes are independently rotated through desirable angles by two DC motors and gears which provides the required actuating torque [5]. Camera stabilizers have complex couplings and completely non-linear dynamic equations in the form of multi-input/multi-output under uncertainties [6]. In a camera stabilizer, there are extra nonlinearities that make the stabilization task more difficult [7]. Due to the complex couplings, non-linear dynamics and the adverse effect of structured and un-structured uncertainties, control of a camera stabilizer is a challenging problem. For applying the controllers on the camera stabilizer and other gimbaled systems as flight motion simulators, at first, these systems have to be linearized and then controlled using linear control design methods [8, 9].

Camera stabilization controllers generally use classical PID. Although the PID framework solves many control problems and is sufficiently flexible to incorporate additional capabilities, it is reported that many PID feedback loops are poorly adjusted. In addition, these control strategies are known to lack adaptability and robustness against changes in the operation environment [10]. In the literature, several improvements to PID controllers are provided [11-13]. For example, in order to decrease accumulating integration error, which causes actuator saturation, self–adjusting integral action is developed. In these approaches, experimental results illustrate that this self-tuning method yields higher precision and perfect control performance under linearity; however, serious disadvantages exist since nonlinear distortion destructs stability in such systems [13]. According to the above description, the controller based on the linear approximation model has good control performance around the set work point. However, when the system is set away from the work point, the system function will deteriorate sharply, and even the instability will occur.

According to the above descriptions, to avoid the disadvantages of the control based on the linear approximation model and to overcome the extant uncertainties, variable structure control to be introduced. Variable structure control (VSC) as one of the nonlinear control methods was first proposed in the early 1950's [14]. The dominant role in VSC theory is played by sliding modes, and the core idea of designing VSC control algorithms consists of enforcing this type of motion in some manifolds in system state spaces [15]. Sliding mode control (SMC) is a nonlinear control technique featuring remarkable properties of accuracy, robustness and easy tuning and implementation. Due to sliding mode control's capability in facing model uncertainties and system disturbances, it has attracted considerable attention in controlling uncertain nonlinear gimbaled systems [16-18]. Despite these advantages, very often, a sliding mode controller yields high-frequency switching control action that leads to the so-called chattering effect, which is difficult to avoid or attenuate [16, 19]. This chattering leads to activation of the system's dynamic modes which in turn reduces the performance of control input [20].

Fuzzy logic in sliding mode control design has been commonly used for numerous electrical systems, robotic systems and mechanical systems in recent years. A direct benefit of the fuzzy sliding mode control in controlling of gimbaled and robotic systems is that the chattering often existing in conventional sliding mode control can be effectively eliminated through construction of fuzzy boundary layers instead of crisp switching surfaces [21-25]. Afterwards, to improve the performance of the resulting control scheme, the coefficients of the fuzzy sliding mode controller are determined by using optimization algorithms [26, 27]. In proposed approaches [28, 29], the number of calculations of the control input is low, the amplitude of control input is the optimal, the proposed control capable overcome structured and unstructured uncertainties and it is very simple to design and implement. Despite these benefits, the proposed controllers do not have the mathematical proof of the closed-loop system stability.

At the present time, by combining SMC, fuzzy logic, and adaptive control concepts, the adaptive fuzzy sliding mode control (AFSMC) has been presented for controlling a class of nonlinear systems [30-32]. By proposing these solutions, the adverse phenomenon of chattering is eliminated at the control input and the researchers have proven that the closed-loop system with adaptive fuzzy sliding mode control has global asymptotic stability in the presence of structured and un-structured uncertainties in the dynamic equations of this category of nonlinear systems. By examining camera stabilizer dynamic equations and comparing them with the dynamic equations of this category of nonlinear systems, it is concluded that some of the proposed approaches can be used to control the camera stabilizer. In this case, by proposing an adaptive fuzzy sliding mode control for controlling camera stabilizer, the following results can be obtained:

[Downloaded from jiaeee.com on 2026-09-13]

[DOR: 20.1001.1.26765810.1396.14.4.3.0]

1. Elimination of unfavorable phenomenon of chattering in the control input.
2. Proof of global asymptotic stability of the closed-loop system in the presence of structured and un-structured uncertainties in the dynamic equations of the camera stabilizer.
3. In adaptive fuzzy sliding mode controllers, an adaptive fuzzy approximator approximates the bounds of the existing uncertainties. Therefore, the input coefficients of the control is updated online and the input control amplitude is placed in an acceptable range. As a result, the costs of practical implementation of the proposed control are decreased.
4. Reduction of the coupling effect in the camera stabilizer, and as a result, reduction of tracking error and an increase in the accuracy of camera stabilizer performance.

Although we can achieve the aforementioned advantages using the adaptive fuzzy sliding mode control. The various techniques of adaptive fuzzy sliding mode control that are presented so far have several merits and demerits; moreover, in some cases, they are not implemental for controlling the camera stabilizer.

In [33], an AFSMC controller has been presented to overcome the existing uncertainties in a nonlinear system. In this method, two adaptive type-2 fuzzy systems have been used to estimate unknown functions. Simulation results show that the proposed control has a good performance in overcoming the existing uncertainties and it makes the tracking error converge to zero. Research shows although the type-2 fuzzy logic is very flexible in overcoming the existing uncertainties in a camera stabilizer, it greatly increases the computational burden of the control input. As a result, there are some problems with the practical implementation of the proposed controller.

An AFSMC controller has been designed in [34]. The proposed approach is only capable of overcoming parametric uncertainties, but, in addition to parametric uncertainties, camera stabilizer encounter un-structured uncertainties and external disturbances. The AFSMC controllers are also presented in [35-37]. Simulation results and mathematical proof show the desirable performance of the proposed controller. However, in the proposed approaches, many adaptive fuzzy systems have been used to estimate the unknown functions of nonlinear systems. Therefore, the control input has a high computational burden. Therefore in case of using this method for control of camera stabilizer, if a delay occurs during the calculation of the control input, it will be impossible to guarantee the stability of the closed-loop system.

In addition to above subjects, like many of the mechatronic and robotic systems [38, 39], the reality is that the camera stabilizer is set up using actuators. Thus to control the camera stabilizer, the actuators must be controlled [40]. This standpoint converts the problems of camera stabilizer control to that of actuator control. For this reason, in this paper a voltage-based AFSMC method is presented for controlling camera stabilizer.

In this paper, it is attempted to propose solutions having the following advantages:

1. Its design steps should be easy.
2. The control input should be based on voltage. In other words, in the design of the proposed control the dynamic equations of the camera stabilizer actuators should be considered.
3. It should have the ability to overcome every type of uncertainty existing in the dynamic equations of the camera stabilizer such as parametric uncertainties, un-modeled dynamics and external disturbances.
4. Single-input, single-output fuzzy rules are used in the proposed approach so that the volume of calculations of the control input are reduced and the number of sensors for the practical implementation of the proposed control is decreased.
5. Chattering is lacking in the amplitude of control input and should be in an allowed range.
6. The number of adaptive rules in the control input should be very few.

This paper is organized as follows: Section 2 describes the statement of the problem and control strategy. In section 3, proposed control methods is introduced in four sub-sections. At first, using dynamic equations of the camera stabilizer as well as using inverse dynamic method, a sliding mode controller is designed. Mathematical proof demonstrates that a closed-loop system with this controller has global asymptotic stability. Next, to eliminate the control input chattering, a first order TSK fuzzy approximator is designed. Despite the ability of the fuzzy sliding mode control in restraining the control input chattering; moreover, the proposed control has some problems such as inability in approximating the bounds of uncertainties as well as lack of stability proof of the closed-loop system. To overcome these problems, an adaptive fuzzy sliding mode control is designed. Afterwards, to determine the optimum coefficients of the adaptive fuzzy sliding mode controller, chicken swarm optimization (CSO) algorithm is used. In section 4, design's process steps of the proposed control is explained. In section 5, to display the performance of the proposed controllers and to compare their function, simulations in four steps are implemented on a camera stabilizer. In section 6, advantages of the proposed control is presented. Ultimately, conclusions of the present research are given in Section 7.

2. Statement of the problem and control strategy

As seen in figure 1, the camera stabilizer has two spinning gimbals perpendicular to each other, namely, inner gimbal and outer gimbal. The outer and inner joints, named the azimuth axis and the elevation axis respectively, both axes are driven by armature-

[Downloaded from jiaeee.com on 2026-09-13]
[DOR: 20.1001.1.26765810.1396.14.4.3.0]

controlled DC motors. Two encoders measure the azimuth and elevation angles. The camera is mounted at the center of the inner joint. The high frequency rotational vibrations can lead to darkness in the camera images, for this reason the inner joint has a freedom to move a few degrees.

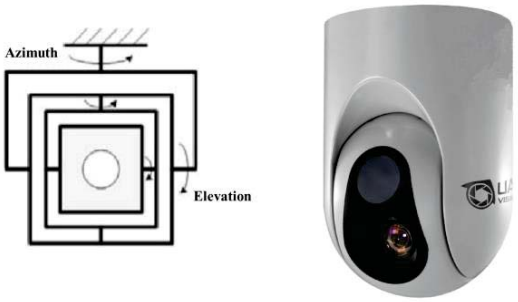

Fig. 1. The two-axis gimbal configuration

Dynamic equations of the camera stabilizer with double-revolute joints including both motor electrical and mechanical dynamic, are expressed as:

$$\begin{cases}(D(q)+r^2J_m)\ddot{q}+(B(q,\dot{q})+r^2B_m)\dot{q}+G(q)+T_d=rK_ri \\ L_{\dot{i}}+Ri+K_m\dot{q}=u,\end{cases} \quad (1)$$

In which:

$$D(q)=\begin{bmatrix} I_{zz}^{C1}+I_{xx}^{C2}sin^2q_2+I_{yy}^{C2}cos^2q_2+I_{xy}^{C2}sin(2q_2) & I_{yz}^{C2}cosq_2-I_{xz}^{C2}sinq_2 \\ I_{yz}^{C2}cosq_2-I_{xz}^{C2}sinq_2 & I_{zz}^{C2}\end{bmatrix}, \quad (2)$$

$$B(q,\dot{q})=\begin{bmatrix} \dot{q}_2(I_{xx}^{C2}sin(2q_2)-I_{yy}^{C2}sin(2q_2)+2I_{xy}^{C2}cos(2q_2)) & -\dot{q}_2(I_{yz}^{C2}sinq_2+I_{xz}^{C2}cosq_2) \\ -\frac{1}{2}\dot{q}_1((I_{xx}^{C2}-I_{yy}^{C2})sin(2q_2)+2I_{xy}^{C2}cos(2q_2)) & 0\end{bmatrix} \quad (3)$$

Where $q(t)\in R^2$ is the vector of joint positions, $\dot{q}(t)\in R^2$ is the vector of joint velocities, $\ddot{q}(t)\in R^2$ is the vector of joint accelerations, $i\in R^2$ is the vector of armature currents, $D(q)\in R^{2\times2}$ is the inertia matrix, which is symmetric and positive-definite, $B(q,\dot{q})\in R^{2\times2}$ represents the centrifugal and Coriolis forces, I_{zz}^{C1} is one of the moment of inertia of link 1 matrix entries with respect to its center of mass, I_{xx}^{C2} , I_{xy}^{C2} , I_{xz}^{C2} , I_{yy}^{C2} , I_{yz}^{C2} and I_{zz}^{C2} are the entries of matrix of moment of inertia of link 2 with respect to its center of mass, $G(q)\in R^2$ is the gravitation vector, which due to the symmetrical structure of the system, its elements are zero, $T_d\in R^2$ is a vector including disturbances or un-modeled dynamics, J_m is the actuator and gear inertia matrix, B_m is the diagonal matrix of damping coefficient, L is the armature inductance matrix, R is the armature resistance matrix, K_m is the diagonal matrix of motor torque constant, K_r is the matrix which characterizes the electromechanical conversion between current and torque, r is the gear ratio matrix and $u\in R^2$ is the armature voltages vector. With respect to second part of the equation (1) we obtain:

$$\dot{i}=\frac{u}{R}-\frac{L}{R}L_{\dot{i}}-\frac{K_m}{R}\dot{q}\,, \quad (4)$$

Equation (4) in the first part of the equation (1) is substituted as:

$$(D(q)+r^2J_m)\ddot{q}+(B(q,\dot{q})+r^2B_m)\dot{q}+G(q)+T_d = rK_r(\frac{u}{R}-\frac{L}{R}L_{\dot{i}}-\frac{K_m}{R}\dot{q})\,, \quad (5)$$

Equation (5) is simplified as:

$$\frac{rK_r}{R}u=(D(q)+r^2J_m)\ddot{q}+\left(B(q,\dot{q})+r^2B_m+\frac{rK_rK_m}{R}\right)\dot{q}+\frac{rK_rL}{R}L_{\dot{i}}+G(q)+T_d\,, \quad (6)$$

For simply more, $W=\frac{rK_r}{R}$, $M(q)=D(q)+r^2J_m$, $C(q,\dot{q})=B(q,\dot{q})+r^2B_m+\frac{rK_rK_m}{R}$ and $H(q,\dot{q})=\frac{rK_rL}{R}L_{\dot{i}}+G(q)+T_d$ are defined. Where $W\in R^{2\times2}$ is a diagonal matrix. By the mentioned substituting, equation (6) is simplified as:

$$u=W^{-1}\left(M(q)\ddot{q}+C(q,\dot{q})\dot{q}+H(q,\dot{q})\right)\,, \quad (7)$$

Equation (7), has the following specifications:

Specifications 1: inertia matrix $M(q)$ is symmetric and positive-definite.

Specifications 2: $\dot{M}(q)-2C(q,\dot{q})$ is a skew-symmetric matrix, as follows:

$$x^T\dot{M}(q)x=2x^TC(q,\dot{q})x \quad , \quad \forall x,q,\dot{q}\in R^2\,. \quad (8)$$

In this system, outer and inner joints of the camera stabilizer is driven by a permanent magnet dc motor. The executed torque on the joint to drive the camera stabilizer is the load torque of motor. According to this concept, the dynamic equation can be considered as [38]:

$$T_m=J_m\ddot{q}_m+B_m\dot{q}_m+\frac{1}{r}T, \quad (9)$$

Where T_m is the motor torque, T is the load torque and q_m is the rotor position. The gear ratio relates the position of motor to the joint position as follow:

$$q=\frac{1}{r}q_m\,, \quad (10)$$

According to the following equation, torque of the motor is proportional to the armature current [41]:

$$T_m=K_ri\,, \quad (11)$$

According to the first and second order derivatives of equation (10) and by substituting equation (11) in (9) we obtain:

$$rK_ri=r^2J_m\ddot{q}+r^2B_m\dot{q}+T, \quad (12)$$

In which:

$$T=D(q)\ddot{q}+B(q,\dot{q})\dot{q}+G(q)+T_d\,. \quad (13)$$

Based on equations (9) to (13), we can plot the general schematic of the system along the controller according to figure 2. As seen in figure 2, control strategy is based on the control of the motor voltage of each joint. The desired trajectories q_{1d} , q_{2d} and their first and second order derivatives are preset for controller while the joint positions q_1 , q_2 and their first order derivative and the motor current i are feedbacks to controller in the real time processing.

[Downloaded from jiaeee.com on 2026-09-13]
[DOR: 20.1001.1.26765810.1396.14.4.3.0]

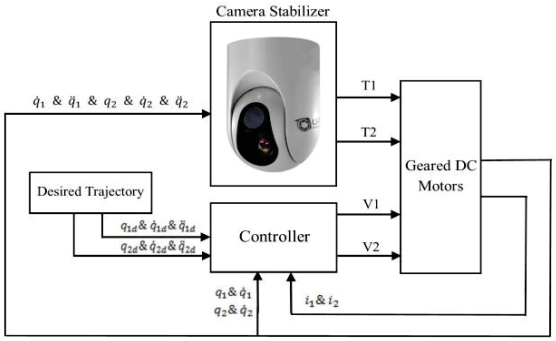

Fig. 2. The camera stabilizer control system

After the general schematic of the system is determined, in the next section, a controller for this system is designed in four steps according to a consolidated procedure.

3. Proposed control methods

The dynamic equations of the camera stabilizer is extremely non-linear and due to existence of the coupling between joints 1 and 2, the design of the controller for this system is difficult. On the other hand, due to existence of uncertainties such as un-modeled dynamics, disturbances and unknown parameters, it is difficult to propose a precise dynamic model for the camera stabilizer [5, 6]. For this reason, the use of a nonlinear robust controller for controlling this system can be considered as an appropriate choice. In this section of the present paper, the method of sliding mode control which is one of the mostly applied methods of nonlinear robust control is utilized.

3.1. Design of sliding mode control

To robust control of the camera stabilizer, the sliding mode controller is designed. Consider a sliding surface vector described as follows [42]:

$$S(t) = (^{d}/_{dt} + \lambda)e\,, \tag{14}$$

In equation (14), $e = q - q_d$ is the tracking error vector in which $q = [q_1\ q_2]^T$ is the vector of joint positions and $q_d = [q_{1d}\ q_{2d}]^T$ is the vector of desired trajectories and $\lambda = \mathrm{diag}[\lambda_1, \lambda_2]$ is a diagonal matrix in which λ_1, λ_2 are constant and positive coefficients. Usually, to design sliding mode controller, the variable $q_r^{(n-1)}$ is defined as:

$$q_r^{(n-1)} = q^{(n-1)} - s(t)\,, \tag{15}$$

Inasmuch as the camera stabilizer is expressed by the second order differential equation, hence equation (15) with $n = 2$ is specified as:

$$\dot{q}_r = \dot{q} - s(t)\,, \tag{16}$$

Taking the derivative of the equation (16), we have:

$$\ddot{q}_r = \ddot{q} - \dot{s}(t)\,. \tag{17}$$

Point 1: Inasmuch as q, $\dot{q}$, $\ddot{q}$ and $s(t)$ are 2×1 vectors, therefore $\dot{q}_r$ and $\ddot{q}_r$ are 2×1 vectors.

To design sliding mode controller, according to the equations (16) and (17), equation (7) is modified to:

$$u = W^{-1}\big(M(q)\ddot{q}_r + M(q)\dot{s}(t) + C(q,\dot{q})\dot{q}_r + C(q,\dot{q})s(t) + H(q,\dot{q})\big)\,, \tag{18}$$

Here, the control law on the sliding mode is proposed as:

$$u = \hat{u} - u_s\,, \tag{19}$$

In which case u_s is the switching control law and $\hat{u}$ is determined as:

$$\hat{u} = \widehat{W}^{-1}\left(\widehat{M}(q)\ddot{q}_r + \hat{C}(q,\dot{q})\dot{q}_r + \widehat{H}(q,\dot{q})\right), \tag{20}$$

In fact, in equations (19) and (20), $\widehat{W}^{-1}$, $\widehat{M}(q)$, $\hat{C}(q,\dot{q})$ and $\widehat{H}(q,\dot{q})$ are estimations of W^{-1}, $M(q)$, $C(q,\dot{q})$ and $H(q,\dot{q})$, respectively. Substituting equations (19) and (20) in (18) we have:

$$W^{-1}\big(M(q)\ddot{q}_r + M(q)\dot{s}(t) + C(q,\dot{q})\dot{q}_r + C(q,\dot{q})s(t) + H(q,\dot{q})\big) = \widehat{W}^{-1}\left(\widehat{M}(q)\ddot{q}_r + \hat{C}(q,\dot{q})\dot{q}_r + \widehat{H}(q,\dot{q})\right) - u_s\,, \tag{21}$$

Equation (21) is simplified, in four steps, as:

$$\big(M(q)\ddot{q}_r + M(q)\dot{s}(t) + C(q,\dot{q})\dot{q}_r + C(q,\dot{q})s(t) + H(q,\dot{q})\big) = W\widehat{W}^{-1}\left(\widehat{M}(q)\ddot{q}_r + \hat{C}(q,\dot{q})\dot{q}_r + \widehat{H}(q,\dot{q})\right) - Wu_s\,, \tag{22}$$

$$M(q)\dot{s}(t) + C(q,\dot{q})s(t) = (W\widehat{W}^{-1}\widehat{M}(q) - M(q))\ddot{q}_r + (W\widehat{W}^{-1}\hat{C}(q,\dot{q}) - C(q,\dot{q}))\dot{q}_r + (W\widehat{W}^{-1}\widehat{H}(q,\dot{q}) - H(q,\dot{q})) - Wu_s\,, \tag{23}$$

$$M(q)\dot{s}(t) + C(q,\dot{q})s(t) = (W\widehat{W}^{-1}\widehat{M}(q) - M(q))\ddot{q}_r + (W\widehat{W}^{-1}\hat{C}(q,\dot{q}) - C(q,\dot{q}))\dot{q}_r + (W\widehat{W}^{-1}\widehat{H}(q,\dot{q}) - H(q,\dot{q})) - Wu_s + u_s - u_s\,, \tag{24}$$

$$M(q)\dot{s}(t) + C(q,\dot{q})s(t) = (W\widehat{W}^{-1}\widehat{M}(q) - M(q))\ddot{q}_r + (W\widehat{W}^{-1}\hat{C}(q,\dot{q}) - C(q,\dot{q}))\dot{q}_r + (W\widehat{W}^{-1}\widehat{H}(q,\dot{q}) - H(q,\dot{q})) - (1-W)u_s - u_s\,, \tag{25}$$

To simplify the mentioned equations, $\Delta M(q) = W\widehat{W}^{-1}\widehat{M}(q) - M(q)$, $\Delta C(q,\dot{q}) = W\widehat{W}^{-1}\hat{C}(q,\dot{q}) - C(q,\dot{q})$, $\Delta H(q,\dot{q}) = W\widehat{W}^{-1}\widehat{H}(q,\dot{q}) - H(q,\dot{q})$, $\Delta f = \Delta M(q)\ddot{q}_r + \Delta C(q,\dot{q})\dot{q}_r + \Delta H(q,\dot{q}) + (1-W)u_s$ are defined and $u_s = Ksgn(s(t))$ is determined, where in, $K = \mathrm{diag}[k_1, k_2]$ is a positive-definite diagonal matrix. Equation (25) is simplified as:

$$M(q)\dot{s}(t) + C(q,\dot{q})s(t) = \Delta M(q)\ddot{q}_r + \Delta C(q,\dot{q})\dot{q}_r + \Delta H(q,\dot{q}) + (1-W)u_s - Ksgn(s(t)) = \Delta f - Ksgn(s(t)). \tag{26}$$

Point 2: $\Delta f \in R^2$ is a vector including all structured and un-structured uncertainties.

In order to prove closed-loop system stability of equation (26), based on the dynamic features of camera stabilizer, Lyapunov function candidate is proposed as:

[Downloaded from jiaeee.com on 2026-09-13]

[DOR: 20.1001.1.26765810.1396.14.4.3.0]

$$V(s(t)) = \frac{1}{2}s^T(t)M(q)s(t)\,, \quad (27)$$

Taking the derivative of the Lyapunov function in equation (27), we have:

$$\dot{V}(s(t)) = s^T(t)M(q)\dot{s}(t) + \frac{1}{2}s^T(t)\dot{M}(q)s(t)\,, \quad (28)$$

Due to the equation (8), equation (28) is rewritten as:

$$\dot{V}(s(t)) = s^T(t)(M(q)\dot{s}(t) + C(q,\dot{q})s(t))\,, \quad (29)$$

With respect to equations (25) and (29), the following equation is obtained:

$$\dot{V}(s(t)) = s^T(t)[\Delta f - Ksgn(s(t))] = \sum_{i=1}^{2}(s_i(t)[\Delta f_i - K_i sgn(s_i(t))])\,, \quad (30)$$

Due to the equation (30), $s_i(t)$ is the i^{th} entry of sliding surface vectors, Δf_i represents the i^{th} entry of the vector Δf and K_i is the i^{th} entry of the main diagonal of matrix k. To prove closed-loop system stability, equation (30) must be less than zero, as follows:

$$\dot{V}(s(t)) = \sum_{i=1}^{2}(s_i(t)[\Delta f_i - K_i sgn(s_i(t))]) < 0\,, \quad (31)$$

Now, the mentioned equation is satisfied if:

$$K_i > \|\Delta f_i\|\,. \quad (32)$$

As a result, by selecting appropriate K which satisfies equation (32), closed-loop control system will possess the global asymptotic stability.

Point 3: Although the closed-loop system with the sliding mode control has a global asymptotic stability in the presence of the existing uncertainties, due to the use of the sgn(*) function in the control input, the occurrence of the unfavorable chattering phenomenon in the control input is unavoidable. Therefore, the practical implementation of this controller is problematic. For this reason in the next section, a fuzzy system is proposed to eliminate the adverse phenomenon of chattering in control input. This fuzzy system prevents abrupt changes in the control input and eliminates the unfavorable phenomenon of chattering to a great extent.

3.2. Design of fuzzy sliding mode controller

A typical fuzzy system has one or more inputs and a single output. A fuzzy system with multiple outputs could be intended as a combination of several single-output systems [43].

Basically, a fuzzy system consists of four fundamental components. The fuzzifier, the fuzzy rule base, fuzzy inference engine and the defuzzifier. The fuzzification and defuzzification play the role of an interface between the fuzzy systems and the crisp systems. The rule base is composed by a set of ''if . . . then . . .'' rules which can be defined based on human experience. Each of fuzzy rules demonstrates a relationship between the input and output variables. For each fuzzy rule, based on the relationship determined by the rule, the input fuzzy sets are mapped to an output fuzzy set by the inference engine. Next, it combines the fuzzy sets from all the rules that exist in the rule base into the output fuzzy set. Ultimately, this output fuzzy set is translated and changed to a crisp value output by the defuzzification. The TSK fuzzy model was proposed by Takagi, Sugeno and Kang in an effort to develop a systematic approach to generating fuzzy rules from a given input-output dataset. Similarly, a first-order fuzzy TSK system is delineated by fuzzy if-then rules which show the relations between inputs and outputs. Generally, first-order fuzzy TSK control system rules are introduced as:

$$\begin{aligned} &if\ x_1\ is\ A_1^i\ and\ \dots and\ \ x_n\ is\ \ A_n^i\ then \\ &\xi^i = a_0^i + a_1^i x_1 + \cdots + a_n^i x_n\,, \end{aligned} \quad (33)$$

Where in $i = 1,2,\dots,M$ and M is the number of fuzzy rules. ξ^i's are the output of these M fuzzy rules and $a_0^i, a_1^i, \dots, a_n^i$ are constant coefficients. In the following, to design fuzzy sliding mode controller, equation (19) could be stated as:

$$\begin{cases} u_p = \hat{u} + K & ,\ s < 0 \\ u_n = \hat{u} - K & ,\ s > 0 \end{cases}\,, \quad (34)$$

According to equation (34), controller fuzzy rules could be stated as:

$$\begin{aligned} &if\ s\ is\ A_1^1\ and\ u_p\ is\ A_2^1\ and\ u_n\ is\ A_3^1\ then \\ &\xi^1 = a_0^1 + a_1^1 s(t) + a_2^1 u_p + a_3^1 u_n \\ &if\ s\ is\ A_1^2\ and\ u_p\ is\ A_2^2\ and\ u_n\ is\ A_3^2\ then \\ &\xi^2 = a_0^2 + a_1^2 s(t) + a_2^2 u_p + a_3^2 u_n\ , \end{aligned} \quad (35)$$

In the aforesaid relation, $a_0^1 = a_0^2 = a_1^1 = a_2^2 = a_1^2 = a_3^1 = 0$ and $a_2^1 = a_3^2 = 1$ and membership functions will be determined as:

$$A_1^1 = \begin{cases} 1 & ,\ s(t) \le -0.5 \\ 1 - 2(s(t) + 0.5)^2 & ,\ -0.5 \le s(t) \le 0 \\ 2(s(t) - 0.5)^2 & ,\ 0 \le s(t) \le 0.5 \\ 0 & ,\ s(t) \ge 0.5 \end{cases}\,, \quad (36)$$

$$A_1^2 = \begin{cases} 0 & ,\ s(t) \le -0.5 \\ 2(s(t) + 0.5)^2 & ,\ -0.5 \le s(t) \le 0 \\ 1 - 2(s(t) - 0.5)^2 & ,\ 0 \le s(t) \le 0.5 \\ 1 & ,\ s(t) \ge 0.5 \end{cases}\,, \quad (37)$$

$$A_2^1 = A_2^2 = 1\ ,\ lower\ bound\ of\ u \le u_p \le upper\ bound\ of\ u\,, \quad (38)$$

$$A_3^1 = A_3^2 = 1\ ,\ lower\ bound\ of\ u \le u_n \le upper\ bound\ of\ u\,. \quad (39)$$

Point 4: To design the controller for camera stabilizer, designers need to have access to the information of dynamic equations of camera stabilizer. In this case, the uncertainties bound of the dynamic equations of camera stabilizer is specified. As a result, for favorable performance of camera stabilizer, the bound of exerted voltage to motors is specified.

Suppose $x = [s(t), u_p, u_n]^T$ to be input vector of fuzzy TSK system, its output will be determined according to the combination of fuzzy rules (35) and is expressed as:

$$y = \frac{\sum_{i=1}^{2} f^i(x)\xi^i(x)}{\sum_{i=1}^{2} f^i(x)}\,, \quad (40)$$

$f^i(x)$ is the firing strength of the i^{th} rule, that is obtained from the following relation:

[Downloaded from jiaeee.com on 2026-09-13]

[DOR: 20.1001.1.26765810.1396.14.4.3.0]

$$f^i(x) = \mu_{A_1^i}(x_1) * \mu_{A_2^i}(x_2) * \mu_{A_3^i}(x_3)\,, \quad (41)$$

" $*$ " is the marker of a t-norm and $\mu_{A_j^i}(x_j)$ demonstrates the membership degree of the input x_j in the membership function A_j^i from the i^{th} rule. In other words, the output of the fuzzy system could be described by the following equation:

$$y = \xi^T \Psi(x)\,, \quad (42)$$

Where, $\xi = [\xi^1, \xi^2]^T$ is the vector of the centers of the membership functions of y, $\Psi(x) = [\Psi(x)^1, \Psi(x)^2]^T$ represents the vector of the height of the membership functions of y where in:

$$\begin{cases} \Psi(x)^1 = f^1(x)/f^1(x) + f^2(x) \\ \Psi(x)^2 = f^2(x)/f^1(x) + f^2(x)\,. \end{cases} \quad (43)$$

The proposed fuzzy sliding mode control includes some advantages which are mentioned below:

1. The proposed fuzzy system prevents the abrupt changes in the control input and thereby prevents chattering.
2. The rule base of the fuzzy system has only two rules. Therefore, the control input has a small number of calculations.
3. By suitable adjustment of the scaling factors of the fuzzy system inputs, the tracking errors of the joints of camera stabilizer can converge to zero.

Despite the aforementioned advantages, the proposed control has some disadvantages which are as follows:

1. The proposed control is not able to approximate the bounds of the existing uncertainties. In other words, the vector of coefficients *K* is determined based on the information in the system and by the designer. As a result, in case a large vector of coefficients *K* is selected, the amplitude of control input also increases.
2. The proposed fuzzy sliding mode control lacks proof of the closed-loop system stability.

Given the above disadvantages, in the next section of the present paper, an adaptive fuzzy system is designed such that it approximates the bounds of the existing uncertainties and also possesses the proof of the closed-loop system stability.

3.3. Design of adaptive fuzzy sliding mode controller

According to equations (19) and (26), definitely this theme can be deduced that the reason for the occurrence of chattering phenomenon in conventional classic sliding mode control rooted in the existence of the constant coefficient K and the Sign function. With these qualities, assume that the control gain $Ksgn(s(t))$ is replaced by a fuzzy gain P. Henceforth, the new control input could be written as:

$$u = \hat{u} - \alpha - P\,. \quad (44)$$

In equation (44), α is a positive constant. To design the adaptive fuzzy controller, the following candidate Lyapunov function is proposed:

$$V(s(t)) = \frac{1}{2} s^T(t) M(q) s(t)\,, \quad (45)$$

In equation (45), $V(s(t))$ is considered as an indicator of the amount of energy of $s(t)$. The system stability is guaranteed by selection a control law such that $\dot{V}(s(t)) < 0$ and $\dot{V}(s(t)) = 0$ only when $s(t) = 0$. In order to avoid undesirable effects of the system uncertainty and reduce the energy of $s(t)$, a fuzzy gain P is used in the adaptive fuzzy sliding mode control. Equation (45) is differentiated with respect to the time, we have:

$$\dot{V}(s(t)) = s^T(t) M(q) \dot{s}(t) + \frac{1}{2} s^T(t) \dot{M}(q) s(t)\,, \quad (46)$$

According to the equation (8), equation (46) is rewritten as follows:

$$\dot{V}(s(t)) = s^T(M(q)\dot{s}(t) + C(q,\dot{q})s(t))\,, \quad (47)$$

With respect to equations (26), (44) and (47), the following equation is obtained:

$$\dot{V}(s(t)) = s^T(t)[\Delta f - P - \alpha] = \sum_{i=1}^{2}(s_i(t)[\Delta f_i - P_i - \alpha_i])\,, \quad (48)$$

From equation (48), it can be concluded that $\dot{V}(s(t)) < 0$ only if:

$$\begin{cases} P_i < \Delta f_i - \alpha_i & , \quad s_i(t) < 0 \\ P_i > \Delta f_i - \alpha_i & , \quad s_i(t) > 0 \end{cases} \quad (49)$$

In the other words, if $\|s_i(t)\|$ is too small, a smaller value of P_i can further guarantee the system stability. And so on, if $\|s_i(t)\|$ is too large then, a larger value of P_i can further guarantee the closed-loop system stability with adaptive fuzzy sliding mode control. Ultimately, if $s_i(t) = 0$ then, the value of P_i could be selected to be equal to zero.

According to the above description, This concept is similar to the idea of applying the function Sat $(*)$. The difference is that the control gain is different along with the sliding surface at all times. Furthermore, for the sake guarantee that P is able to compensating the disadvantages caused of system uncertainty, an adaptive law is designed. It is clear by these analyses that the value of P could be determined by the value of the sliding surface $s(t)$. With these qualities, the fuzzy system for P must be a SISO system, with $s(t)$ as the input and P as the output variable. The rules in the rule base are in the following specified format:

$$if\ s(t)\ is\ A_i^m\ then\ P\ is\ B_i^m\,, \quad (50)$$

In which A_i^m and B_i^m are fuzzy sets. In this paper, the same type of membership functions, i.e. NB, NM, NS, ZE, PS, PM, PB are selected for both $s(t)$ and P where, N stands for negative, P positive, B big, M medium, S small and ZE zero. These are all Gaussian membership functions defined by considering to the following equation:

$$\mu_A(x_i) = exp[-\left(\frac{x_i - \theta}{\sigma}\right)^2]\,, \quad (51)$$

In which, ''A'' represents one of the fuzzy sets NB, ..., PB and x_i denotes $s(t)$ or P. θ is the center of ''A'' and σ is the width of ''A''. In spite of the fact that the membership functions for $s(t)$ and P have the similar titles, proportionally, the values of the center and the width of the membership function with a similar title for $s(t)$ and P are different; respectively. The

[Downloaded from jiaeee.com on 2026-09-13]
[DOR: 20.1001.1.26765810.1396.14.4.3.0]

parameters of the membership functions of P are updated online insomuch, those of $s(t)$ have predefined quantities. Therefore, the controller is an adaptive controller.

According to the definitions of the input and output membership functions and base on the above discussed topics, the following rules could be determined as the rule base:

$$\begin{aligned}
&if\ s(t)\ is\ NB\ then\ P\ is\ NB\\
&if\ s(t)\ is\ NM\ then\ P\ is\ NM\\
&if\ s(t)\ is\ NS\ then\ P\ is\ NS\\
&if\ s(t)\ is\ ZE\ then\ P\ is\ ZE\\
&if\ s(t)\ is\ PS\ then\ P\ is\ PS\\
&if\ s(t)\ is\ PM\ then\ P\ is\ PM\\
&if\ s(t)\ is\ PB\ then\ P\ is\ PB\ .
\end{aligned} \tag{52}$$

In addition, on the basis of our knowledge of fuzzy systems and considering the equations (40) and (42), fuzzy gain P can be written as follows:

$$P = \frac{\sum_{i=1}^{M} \xi^i \mu_{A^i}(s(t))}{\sum_{i=1}^{M} \mu_{A^i}(s(t))} = \xi^T \Psi(s(t)) , \tag{53}$$

Where M is the amount of the rules.
And also, $\xi = [\xi^1, \cdots, \xi^i, \cdots, \xi^M]^T$, $\Psi(s(t)) = [\Psi(s(t))^1, \cdots, \Psi(s(t))^i, \cdots, \Psi(s(t))^M]^T$ and $\Psi(s(t))^i$ denoted as follows:

$$\Psi(s(t))^i = \prod_{j=1}^{n} \mu_{A_j^i}(s(t)) / \sum_{i=1}^{M} \prod_{j=1}^{n} \mu_{A_j^i}(s(t)) . \tag{54}$$

ξ is chosen as a parameter to be updated and for this reason it is called the parameter vector. $\Psi(s(t))$ is known as the function basis vector and can be intended as the weight of the parameter vector. Next, define ξ^* so $P = \xi^{*T}\Psi(s(t))$ is the optimal compensation for Δf. According to the Wang's theorem [43], there exists $\beta > 0$ which satisfies the following inequality:

$$\Delta f - P = \Delta f - \xi^{*T}\Psi(s(t)) < \beta , \tag{55}$$

In the mentioned inequality, β is approximation error and it can be as small as possible. After that, define:

$$\tilde{\xi} = \xi - \xi^* , \tag{56}$$

According to equations (53) and (56) it is concluded that:

$$P = \tilde{\xi}^T \Psi(s(t)) + \xi^{*T}\Psi(s(t)) . \tag{57}$$

When all the details of designing adaptive fuzzy control are analyzed, for the design it, the candidate Lyapunov function is modified and the equation (45) is rewritten as follows:

$$V(s(t)) = \frac{1}{2} s^T(t) M(q) s(t) + \frac{1}{2\varepsilon} \tilde{\xi}^T \tilde{\xi} , \tag{58}$$

In which, ε is a constant parameter that is greater than zero. Equation (58) is differentiated with respect to the time and the following equation is obtained:

$$\dot{V}(s(t)) = s^T(t) M(q) \dot{s}(t) + \frac{1}{2} s^T(t) \dot{M}(q) s(t) + \frac{1}{2\varepsilon} (\dot{\tilde{\xi}}^T \tilde{\xi} + \tilde{\xi}^T \dot{\tilde{\xi}}) , \tag{59}$$

Based on equations (8), (47) and (48), simplifying equation (59) results in:

$$\dot{V}(s(t)) = s^T(t)[\Delta f - P - \alpha] + \frac{1}{\varepsilon} \tilde{\xi}^T \dot{\xi} , \tag{60}$$

Equation (57) is substituted in equation (60) and the result is rewritten as follows:

$$\dot{V}(s(t)) = s^T(t)[\Delta f - \tilde{\xi}^T \Psi(s(t)) - \xi^{*T}\Psi(s(t)) - \alpha] + \frac{1}{\varepsilon} \tilde{\xi}^T \dot{\xi} , \tag{61}$$

Then, equation (61) is reorganized as follows:

$$\dot{V}(s(t)) = s^T(t)[\Delta f - \xi^{*T}\Psi(s(t)) - \alpha] + \tilde{\xi}^T \left[\frac{1}{\varepsilon} \dot{\xi} - s^T(t)\Psi(s(t))\right] , \tag{62}$$

According to equation (62), the adaptive rule could be selected as follows:

$$\dot{\xi} = \varepsilon s^T(t) \Psi(s(t)) , \tag{63}$$

By choosing the aforementioned adaptive rule, equation (62) is simplified as follows:

$$\dot{V}(s(t)) = s^T(t)[\Delta f - \xi^{*T}\Psi(s(t)) - \alpha] , \tag{64}$$

With respect to equations (55) and (64) it is concluded that:

$$\dot{V}(s(t)) < (\beta - \alpha) \| s^T(t) \| , \tag{65}$$

Equation (65) demonstrates that by properly choosing the coefficient α, $\dot{V}(s(t)) < 0$ is satisfied. Accordingly, the closed-loop system with adaptive fuzzy sliding mode control is globally asymptotically stable in presence of all structured and unstructured uncertainties. Finally, to summarize our discussion, the proposed control input is expressed as follows:

$$\begin{cases} u = \hat{u} - \alpha - P \\ \hat{u} = \widehat{W}^{-1} \left(\widehat{M}(q) \ddot{q}_r + \hat{C}(q, \dot{q}) \dot{q}_r + \hat{H}(q, \dot{q}) \right) \\ P = \xi^T \Psi(s(t)) \\ \dot{\xi} = \varepsilon s^T(t) \Psi(s(t)) . \end{cases} \tag{66}$$

Point 5: In the proposed control, although the vector P is updated during the control of the camera stabilizer, there are coefficients such as α, ε and the coefficients of the sliding surfaces in the proposed control which should still be adjusted using trial and error method. The suitable choice of these coefficients has a considerable effect on the reduction of the tracking error as well as the amplitude of control input. Therefore, in the next section, it is attempted to adjust these coefficients via chicken swarm optimization algorithm.

3.4. Chicken Swarm Optimization Algorithm

In this section, a novel bio-inspired algorithm, Chicken Swarm Optimization (CSO) [44], is studied. To mathematical development of the CSO, chickens' behaviors is idealized by the rules stated below:

1. Several groups is available in the chicken swarm. Each group possesses a predominant rooster, a pair of hens and chicks.
2. How to distribute the chicken swarm to various groups and specify the certain identity of the chickens (roosters, hens and chicks) all depending on the physical fitness values of the chickens themselves. The chickens with best various

[Downloaded from jiaeee.com on 2026-09-13]
[DOR: 20.1001.1.26765810.1396.14.4.3.0]

physical fitness values would be acted as roosters, either one of which would be the head rooster in a specified group. The chickens with weakest fitness values would be determinate as chicks. All the others would be hens. The hens at random select which group to live in. The mother-child relationship between the hens and the chicks is as well as accidentally specified.

3. The hierarchical regularity, overlord relationship and mother and child relationship in a group will remain without changes. These situation just update every various (G) time steps.
4. Chickens pursue their group- helpmate rooster to seek food, whereas they may rebuff the ones from eating their own food. Consider chickens would at random grab the good food formerly obtain by others. The chicks search for food surrounding their mother. The predominant individuals have excellence in rivalry for food.

Suppose RN, HN, CN and MN demonstrate the number of the roosters, the hens, the chicks and the mother hens, respectively. The best RN chickens would be supposed to be roosters, whereas the weakest CN ones would be considered like chicks. Others are under treatment, as hens. All N figurative chickens, portrayed by their special positions $x_{i,j}^{t}$ ($i \in [1, \dots, N], j \in [1, \dots, D]$) at time step t, looking for food in a D-dimensional space. In these situations, the optimization problems are the minimal of those. Hence, the best RN chickens is equivalent to the ones with RN minimal physical fitness values. The roosters with superior physical fitness values have precedence for food accessibility than the ones with worse physical fitness values. To simplify the expression of issue, this item can be simulated with the condition that the roosters with better physical fitness values can looking for food in a broader range of places than that of the roosters with weakest fitness values. This can be formulated as:

$$x_{i,j}^{t+1} = x_{i,j}^{t} * \left(1 + Randn(0, \nabla^2)\right) . \quad (67)$$

$$\nabla^2 = \begin{cases} 1 & , \quad if \quad f_i \le f_k \\ exp\left(\frac{(f_k - f_i)}{|f_i| + \Gamma}\right) & , \quad otherwise \end{cases} ; \; k \in [1, N], k \ne i \; . \quad (68)$$

Which $Randn(0, \nabla^2)$ is a gaussian distribution with mean 0 and standard deviation ∇^2. Γ which is utilized to prevent zero-division-error, is the smallest constant value in the computer. k a rooster's indicator, is at random chosen from the roosters group, f is the physical fitness value of the corresponding x parameter.

But about the hens, they can pursue their group-helpmate roosters to looking for food. Furthermore, they would also haphazardly rob the good food detected by other chickens, although they would be suppressed by other chickens. The more prominent hens would have benefit in competition for food than the more docile ones. These expressed phenomenon can be formulated mathematically as follows:

$$x_{i,j}^{t+1} = x_{i,j}^{t} + Z_1 * Rand * (x_{r_1,j}^{t} - x_{i,j}^{t}) + Z_2 * Rand * (x_{r_2,j}^{t} - x_{i,j}^{t}) \; . \quad (69)$$

$$Z_1 = exp((f_i - f_{r_1}) / (abs(f_i) + \Gamma)) \; . \quad (70)$$

$$Z_2 = exp(f_{r_2} - f_i) \; . \quad (71)$$

In which Rand is a monotone random number in the range of [0, 1]. $r_1 \in [1, \dots, N]$ is an indicator of the rooster, which is the i[th] hen's group-helpmate, while $r_2 \in [1, \dots, N]$ is an indicator of the chicken (hen or rooster), which is at random selected from the swarm. $r_1 \ne r_2$. It is obvious that, $f_i > f_{r_1}$ and $f_i > f_{r_2}$ thus $Z_2 < 1 < Z_1$. Suppose $Z_1 = 0$, then the i[th] hen would fodder for food only followed by another chickens. The paramount the difference of the two chickens' physical fitness values, the lesser Z_2 and the bigger the split between the two chickens' positions is. Therefore the hens would not comfortably rob the food found by another chickens. The sake that the formula form of Z_1 distinct from that of $Z_2 = 0$ is that there exist rivalries in a group. For simplicity's sake, the physical fitness values of the chickens compared to the physical fitness value of the rooster are simulated as the rivalries between chickens in a group. Suppose $Z_2 = 0$, then the i[th] hen would fodder for food in their own scope. For the specified group, the rooster's physical fitness value is distinctive. Therefore the lesser the i[th] hen's physical fitness value, the closer Z_1 approaches to 1and the lesser the split between the positions of the i[th] hen and its group-helpmate rooster is. Therefore the more predominant hens would be more probable than the more docile ones to eat the food. The chickens move around their mother to fodder for food. This concept is formulated as follows:

$$x_{i,j}^{t+1} = x_{i,j}^{t} + FL * (x_{m,j}^{t} - x_{i,j}^{t}) \; . \quad (72)$$

In which $x_{m,j}^{t}$ signify the position of the i[th] chick's mother($m \in [1, N]$). $FL(FL \in (0,2))$ is a parameter, which denotes that the chick would pursue its mother to fodder for food. Consider the exclusive distinctions, the FL of each chick would at random choose between 0 and 2. The framework of the CSO is expressed in [44].

4. Design's process steps of the proposed control

In this section of the paper, the details of implementation of the proposed control is discussed. To implement this control method, the following steps should be pursued:

1. Determination of the tracking errors $e_1(t)$ and $e_2(t)$.
2. Determination of the sliding surfaces, through the initial choice of the constant and positive values of λ_1 and λ_2.
3. Determination of $\dot{q}_r$ and $\ddot{q}_r$ through equations (16) and (17).
4. Determination of the estimated dynamics $\widehat{W}^{-1}$, $\widehat{M}(q)$, $\widehat{C}(q, \dot{q})$ and $\widehat{H}(q, \dot{q})$. In this case, the vector $\hat{u}$ in the input of the proposed control is determined.

[Downloaded from jiaeee.com on 2026-09-13]
[DOR: 20.1001.1.26765810.1396.14.4.3.0]

5. Initial determination of the constant and positive coefficient ε_1 and ε_2.
6. Determination of the membership functions of the sliding surfaces and determination of $\Psi(s(t))^i$ through equation (54). In this case, the vector $\Psi(s(t))$ is determined.
7. Determination of the vector ξ through integrating equation (63).
8. Determination of the vector P through equation (53) and initial determination of the vector of coefficients α according to the information available from the bounds of the uncertainties of the system.
9. Use of chicken swarm optimization algorithm to re-determine the optimal values from the entries of the vectors λ, ε and α.

5. Simulation results

In this section of the paper, simulations in four steps are applied on the camera stabilizer to investigate the performance of the proposed controllers. In these simulations, the matrix of the inertia moment of the links 1 and 2 is considered according to table 1.

Table. 1. Moment of inertia matrices of camera stabilizer links

Moments of inertia matrix of link 1 I^{C1}	$\begin{bmatrix} 4.0088 & 0.0124 & 0.0469 \\ 0.0124 & 4.4970 & 0.0092 \\ 0.0469 & 0.0092 & 2.5414 \end{bmatrix} Kg.m^2$
Moments of inertia matrix of link 2 I^{C2}	$\begin{bmatrix} 0.1104 & 0 & -0.0116 \\ 0 & 0.1117 & 0 \\ -0.0116 & 0 & 0.0074 \end{bmatrix} Kg.m^2$

Furthermore, the parameters of the electrical motors 1 and 2 are specified according to Table 2. It is worth remembering that the angular position of the electrical motor 1 determines azimuth angle and the angular position of the electrical motor 2 determines angle of sight.

Table. 2. Parameters of permanent magnet dc motors

$J_{m_1} = 0.000146$	$J_{m_2} = 0.0001$	$\hat{J}_{m_1} = 0.000155$	$\hat{J}_{m_2} = 0.00011$
$B_{m_1} = 0.2276$	$B_{m_2} = 0.0721$	$\hat{B}_{m_1} = 0.2286$	$\hat{B}_{m_2} = 0.0732$
$K_{m_1} = 119$	$K_{m_2} = 25.6$	$\hat{K}_{m_1} = 125$	$\hat{K}_{m_2} = 28.6$
$K_{r_1} = 2.7$	$K_{r_2} = 0.274$	$\hat{K}_{r_1} = 2.8$	$\hat{K}_{r_2} = 0.288$
$R_1 = 0.176$	$R_2 = 0.4695$	$\hat{R}_1 = 0.186$	$\hat{R}_2 = 0.47$
$r_1 = 0.011$	$r_2 = 0.178$	$\hat{r}_1 = 0.0111$	$\hat{r}_2 = 0.182$
$L_1 = 0.08$	$L_2 = 0.04$	$\hat{L}_1 = 0.085$	$\hat{L}_2 = 0.045$

Point 6: $\hat{J}_{m_1}$, $\hat{J}_{m_2}$, $\hat{B}_{m_1}$, $\hat{B}_{m_2}$, $\hat{K}_{m_1}$, $\hat{K}_{m_2}$, $\hat{K}_{r_1}$, $\hat{K}_{r_2}$, $\hat{R}_1$, $\hat{R}_2$, $\hat{r}_1$, $\hat{r}_2$, $\hat{L}_1$ and $\hat{L}_2$ are the estimations from the actual quantities of J_{m_1} , J_{m_2} , B_{m_1} , B_{m_2} , K_{m_1} , K_{m_2} , K_{r_1} , K_{r_2} , R_1 , R_2 , r_1 , r_2 , L_1 and L_2 which have been used in calculation of û.

The assumed values of disturbances or un-modeled dynamics are considered as $T_{d_1} = 5$ and $T_{d_2} = 2$. The quantities of parameters in controller (25) which have been used in this simulation are presented in Table 3.

Table. 3. Parameters of controller (25)

k_1=10	k_2=5
λ_1=50	λ_2=30

5.1. Step 1 of simulation (SMC)

In step 1 of simulation, sliding mode control of equation (25) is applied for camera stabilizer. After performing the simulation, desired and actual trajectories have been shown in figure 3. It is worth mentioning that the desired trajectory begins at $(q_{1_0}, q_{2_0}) = (0, 0)$.

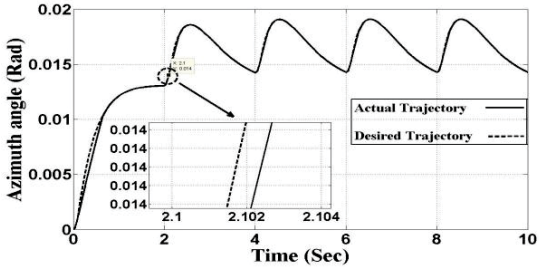

(a) Desired and actual trajectory for azimuth angle

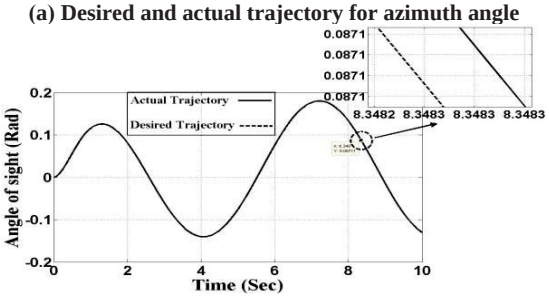

(b) Desired and actual trajectory for angle of sight

Fig. 3. Desired and actual trajectories for joints 1 and 2

[Downloaded from jiaeee.com on 2026-09-13]
[DOR: 20.1001.1.26765810.1396.14.4.3.0]

Tracking errors of joints 1 and 2 are shown in figure 4.

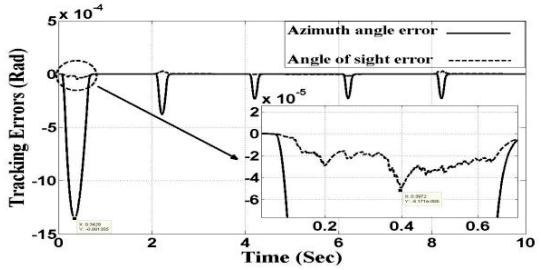

Fig. 4. Tracking errors of the joints 1 and 2, in sliding mode control

According to figures 3 and 4, it is evident that the precise tracking in joints 1 and 2 have been occurred, such that the maximum tracking error for azimuth angle and angle of sight are $13.5 \times 10^{-4}\ Rad$ and $5.17 \times 10^{-5}\ Rad$, respectively. Figure 5 shows control inputs for azimuth and elevation motors.

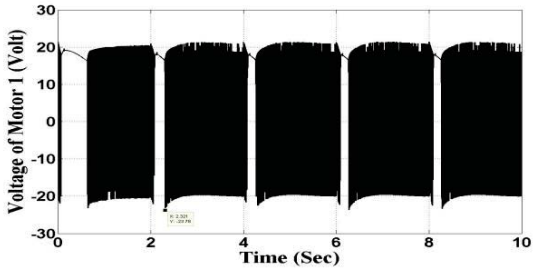

(a) Exerted control input to motor 1

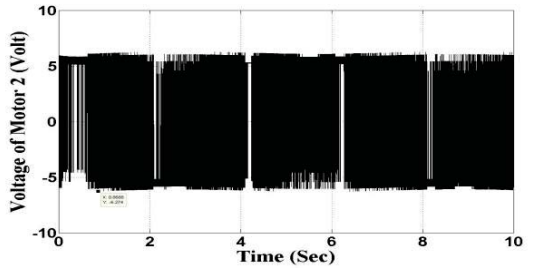

(b) Exerted control input to motor 2

Fig. 5. Exerted control inputs to motors 1 and 2, in sliding mode control

As can be seen in figure 5, the chattering domain of exerted control inputs to motor 1 (azimuth motor) and motor 2 (elevation motor) are 0.26 to 42.17 volts and 0.68 to 12.35 volts, respectively. This chattering can lead to the activation of the nonlinear dynamic modes of the camera stabilizer and erosion of the azimuth and elevation motors, and finally causes instability in the control system and damage to the physical structure of the camera stabilizer. In addition, as it is understood from figure 8, the maximum of input voltage amplitude of motors 1 and 2 are 23.78 volt and 6.27 volt, respectively. In figure 6, the chattering of the sliding surfaces s_1 and s_2 is obvious.

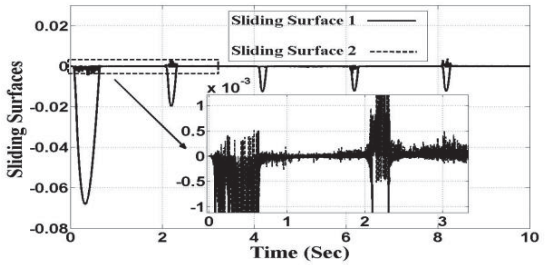

Fig. 6. The sliding surfaces in sliding mode control

According to equations (25), (26) and (32) it is evident that knowing the bounds of structured and un-structured uncertainties (Δf) has a significant role in determining the coefficients of the vector *K* and finally in determining the stability of the closed-loop system. Thus Δf is shown in figure 7.

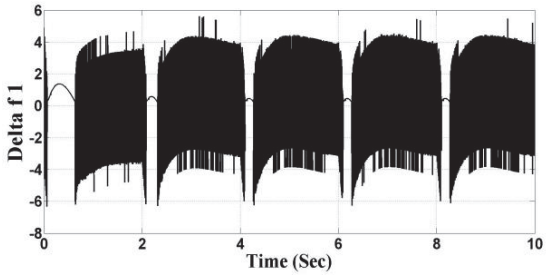

(a) All structured and un-structured uncertainties for joint 1

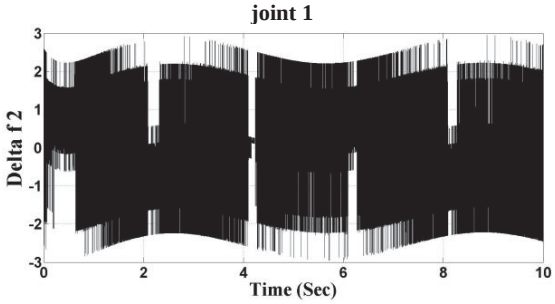

(b) All structured and un-structured uncertainties for joint 2

Fig. 7. All structured and un-structured uncertainties

According to figure 7, it is obvious that the bounds of structured and un-structured uncertainties for the joints 1 and 2 are completely specified. For this reason, the equation of $\|\Delta f_i\|$ can be depicted in joints 1 and 2 as in figure 8.

[Downloaded from jiaeee.com on 2026-09-13]

[DOR: 20.1001.1.26765810.1396.14.4.3.0]

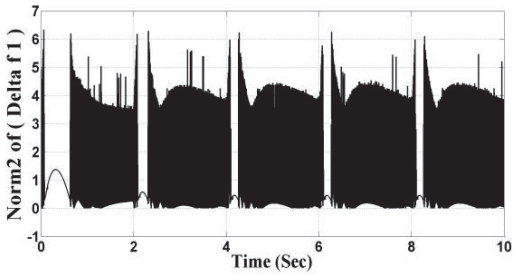

(a) $\|\Delta f_i\|$ for joint 1 (i=1)

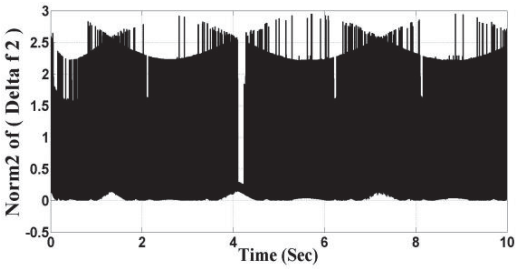

(b) $\|\Delta f_i\|$ for joint 2 (i=2)

Fig. 8. $\|\Delta f_i\|$ for joints 1 and 2 (i=1,2)

According to figure 8 and equation (32), the allowed range for determining the coefficients of the vector K is completely specified. On the other hand, according to table 3 and the values of the control parameters mentioned, it can be concluded that the values of K_1 and K_2 are truly determined and used in the structure of the control system. Next, according to the mentioned values of K_1 and K_2 the diagram of the changes in $Ksgn(s(t))$ in terms of time is plotted in figure 9.

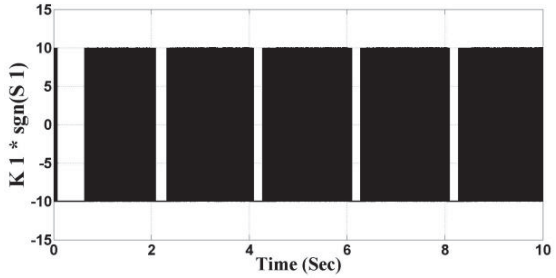

(a) The control gain $K_1 sgn(s_1(t))$

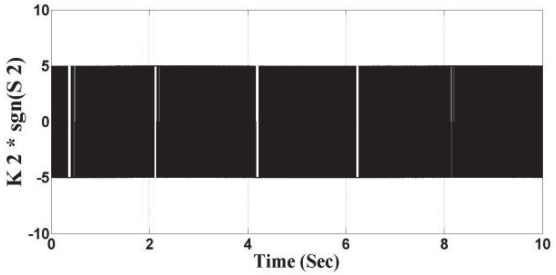

(b) The control gain $K_2 sgn(s_2(t))$

Fig. 9. The control gain $Ksgn(s(t))$, in sliding mode control

According to figure 9, high chattering and non-smooth variations in the diagrams of $K_1 sgn(s_1(t))$ and $K_2 sgn(s_2(t))$ is observed. In the next step of simulation, to overcome the adverse chattering phenomenon in control inputs, fuzzy sliding mode control input is applied and simulated for camera stabilizer.

5.2. Step 2 of simulation (FSMC)

After applying the fuzzy sliding mode control input to camera stabilizer, simulation is executed. Tracking errors of joints 1 and 2 are shown in figure 10.

By comparing figures 4 and 10, it is obvious that a more precise tracking in comparison with the previous step of simulation is conducted in joints 1 and 2, such that the maximum tracking error in azimuth and elevation are $11 \times 10^{-5}\, Rad$ and $5.1 \times 10^{-6}\, Rad$, respectively. In figure 11, the applied control inputs to the azimuth and elevation motors are displayed.

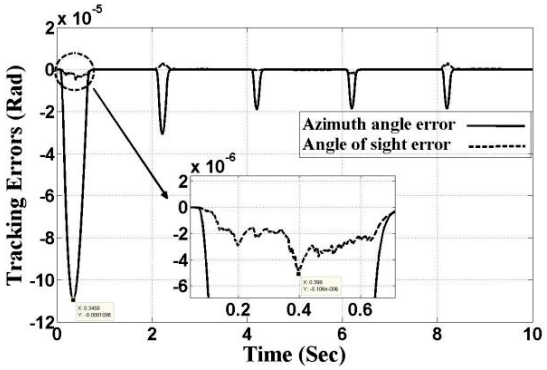

Fig. 10. Tracking errors of the joints 1 and 2, in fuzzy sliding mode control

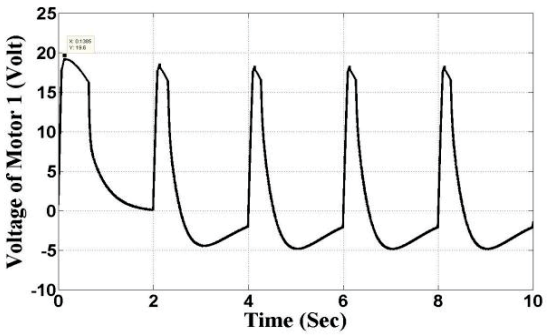

(a) Exerted control input to motor 1

[Downloaded from jiaeee.com on 2026-09-13]

[DOR: 20.1001.1.26765810.1396.14.4.3.0]

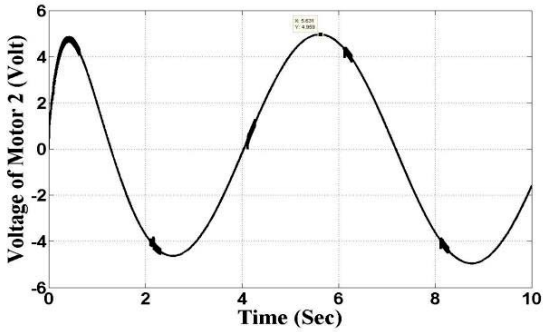

(b) Exerted control input to motor 2

Fig. 11. Exerted control inputs to motors 1 and 2, in fuzzy sliding mode control

According to figure 11, it is observed that the control inputs have negligible chattering in a limited time intervals. In addition, the maximum input voltages of the motors 1 and 2 are $19.6\,Volt$ and $4.96\,Volt$, respectively. According to the remarks stated in section 3-2, the adaptive fuzzy sliding mode control input is applied to the camera stabilizer in the next step of the simulation.

5.3. Step 3 of simulation (AFSMC)

In this step of simulation, according to Table 4, entries of vectors ε and α are adjusted.

Table. 4. Quantities of controlling parameters ε_1 , ε_2 , α_1 and α_2 utilized in adaptive fuzzy sliding mode

ε_1=5	ε_2=52
α_1=4.73	α_2=3.42

After applying input of the adaptive fuzzy sliding mode control to the camera stabilizer, and conducting the simulations, the results are presented as follows:

After performing the simulation, the diagram of the variations in the vector P in terms of time is plotted in figure 12.

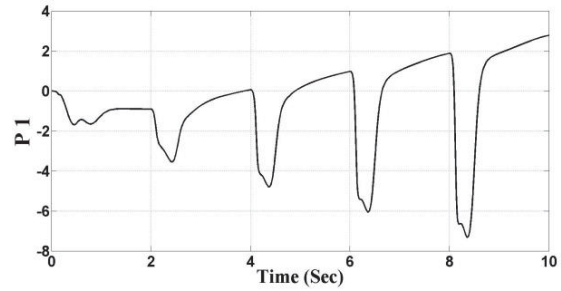

(a) The fuzzy gain P_1

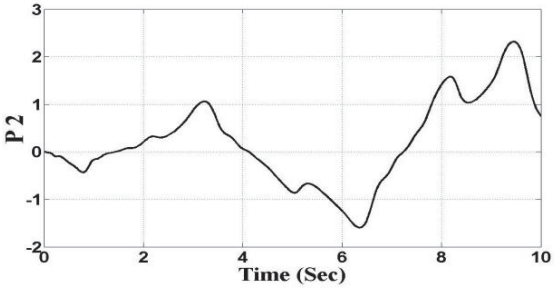

(b) The fuzzy gain P_2

Fig. 12. The fuzzy gain P, in adaptive fuzzy sliding mode control

By comparing figures 9 and 12, lack of chattering and smooth approximation of the control gains P_1 and P_2 is observable. This suitable approximation shows that the adaptive fuzzy system functions satisfactorily and has specified the bounds of the existing uncertainties. Tracking errors of joints 1 and 2 are shown in figure 13.

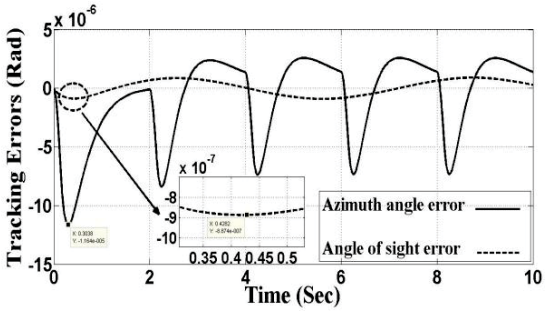

Fig. 13. Tracking errors of the joints 1 and 2, in adaptive fuzzy sliding mode control

By comparing figure 13 with figures 4 and 10, the considerable reduction of the tracking error in this step of the simulations is remarkable. The maximum tracking error in the azimuth is $11.6 \times 10^{-6}\,Rad$ and in the elevation, it is $8.9 \times 10^{-7}\,Rad$. Figure 14 shows exerted control inputs for azimuth and elevation motors.

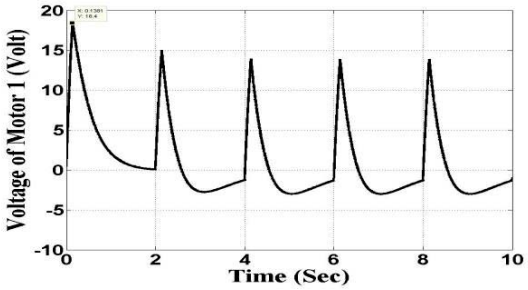

(a) Exerted control input to motor 1

[Downloaded from jiaeee.com on 2026-09-13]

[DOR: 20.1001.1.26765810.1396.14.4.3.0]

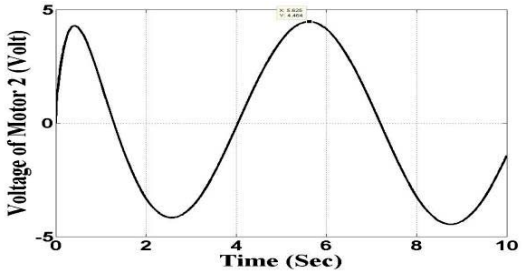

(b) Exerted control input to motor 2

Fig. 14. Exerted control inputs to motors 1 and 2, in adaptive fuzzy sliding mode control

According to figure 14, it is clear that control inputs have no chattering. In addition, the maximum amplitude of the input voltage of motors 1 and 2 are $18.4\,Volt$ and $4.46\,Volt$, respectively. Figure 15 shows the sliding surfaces s_1 and s_2.

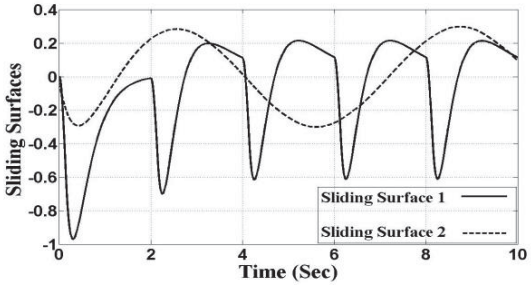

Fig. 15. The sliding surfaces in adaptive fuzzy sliding mode control

By paying attention to figure 15 and comparing it with figure 6, it is evident that the sliding surfaces s_1 and s_2 have no chattering and have smooth vibrations around the zero sliding surface. As was predicted, in this step of the simulations with smooth and desirable approximation of vector *P*, the control targets such as lack of the chattering of the control input and minimum tracking error, to a great extent are more favorable compared to the previous steps of simulation. However, it should be remembered that in addition to the vector *P*, the suitable choice of the coefficients of vector ε can lead to far more precise tracking and lower tracking error. Therefore, to investigate the effect of different values of the vector ε in decreasing the tracking error, different values of the coefficients of the vector ε is used in the adaptive fuzzy sliding mode control of camera stabilizer according to table 5.

Table. 5. Quantities of ε_1 and ε_2 utilized in adaptive rule of equation (63)

1	$\varepsilon_1 = 10$	$\varepsilon_2 = 125$
2	$\varepsilon_1 = 112$	$\varepsilon_2 = 1100$
3	$\varepsilon_1 = 543$	$\varepsilon_2 = 5420$

In three steps, different values of the coefficient of vector ε is applied to the adaptive fuzzy sliding mode control input structure of the camera stabilizer. After executing the simulation, tracking errors of joints 1 and 2 are indicated in figure 16.

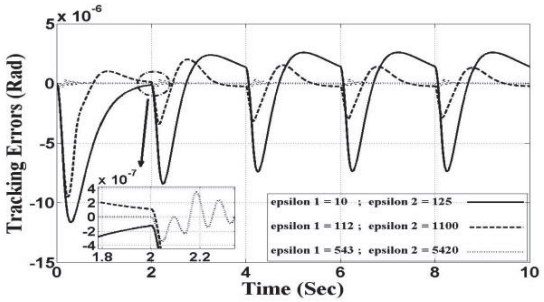

(a) Tracking errors for various quantities of ε_1 and ε_2 in azimuth angle

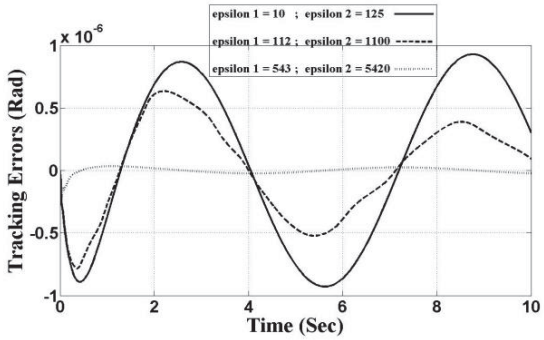

(b) Tracking errors for various quantities of ε_1 and ε_2 in angle of sight

Fig. 16. The tracking errors for various quantities of ε_1 and ε_2 in azimuth angle and angle of sight

By concentrating on figure 16, the reduction of the tracking error in the joints 1 and 2 is observable by the increase in the control coefficients of ε_1 and ε_2. As it is evident, by applying $\varepsilon_1 = 543$ and $\varepsilon_2 = 5420$, the minimum tracking error results is obtained such that in this case, the maximum tracking error is $3.47 \times 10^{-7}\,Rad$ in the azimuth and $3.44 \times 10^{-8}\,Rad$ in the elevation. According to figure 17, by applying these coefficients of the vector ε, despite the considerable reduction in the tracking error, the amplitude of control inputs has not substantially increased.

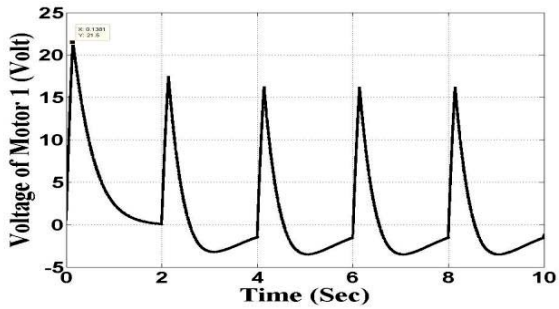

(a) Exerted control input to motor 1

[Downloaded from jiaeee.com on 2026-09-13]

[DOR: 20.1001.1.26765810.1396.14.4.3.0]

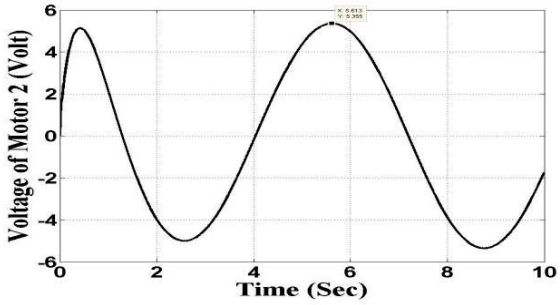

(b) Exerted control input to motor 2

Fig. 17. Exerted control inputs to motors 1 and 2 for $\varepsilon_1 = 543$ and $\varepsilon_2 = 5420$

So far in previous three steps of simulation, a constant quantity of disturbance is applied to the camera stabilizer. In the next step of simulation, to establish more challenges in performance of controller and also to test the robustness of the adaptive fuzzy sliding mode control against disturbances, the control system is challenged and external time varying disturbances are applied to the camera stabilizer.

5.4. Step 4 of simulation (OAFSMC)

In this step of the simulation, to show the impact of control input coefficients on the performance of adaptive fuzzy sliding mode control, the controller parameters ε , λ and α are searched and adjusted in the allowable range by the CSO algorithm. The related parameters of the CSO algorithm are listed in table 6.

Table. 6. The related parameter values of CSO algorithm

$RN = 0.18 * N$	$HN = 0.63 * N$
$CN = N - RN - HN$	$MN = 0.11 * N$
$G = 13$	$FL \in [0.33\ , 0.85]$

The optimal values of control input coefficients are presented in table 7.

Table. 7. Quantities of controlling parameters ε, λ and α utilized in optimal adaptive fuzzy sliding mode

$\varepsilon_1 = 504$	$\varepsilon_2 = 4960$
$\lambda_1 = 39$	$\lambda_2 = 24$
$\alpha_1 = 4.28$	$\alpha_2 = 3.16$

Until now in all steps of simulation, a constant quantity of disturbance ($T_{d_1} = 5$ and $T_{d_2} = 2$), is applied to the camera stabilizer. In this step of the simulation, to test the robustness of the proposed control system against disturbances, the closed-loop control system is challenged and disturbances are applied to the camera stabilizer as indicated in figure 18.

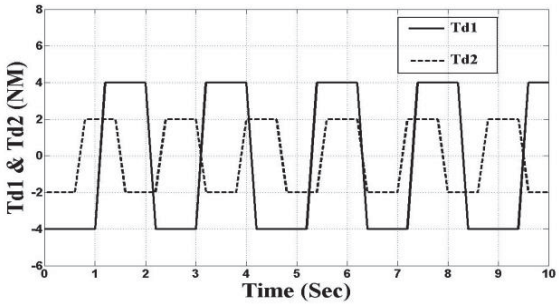

Fig. 18. Exerted challenging disturbances to the camera stabilizer

To clarify the design of the optimal adaptive fuzzy sliding mode control for the camera stabilizer, the diagram block of the closed-loop system is depicted in figure 19.

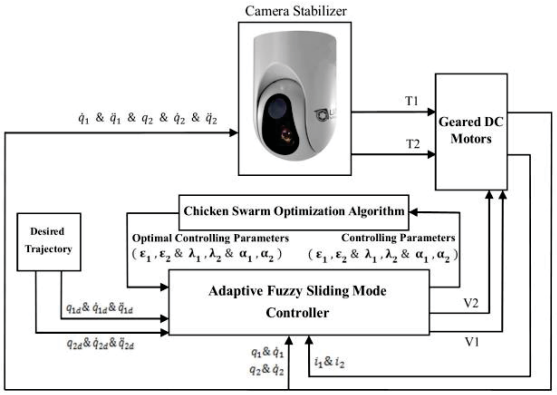

Fig. 19. The schematic diagram of optimal adaptive fuzzy sliding mode control (step 4 of simulation)

After executing the simulation, tracking errors of joints 1 and 2 are shown in figure 20.

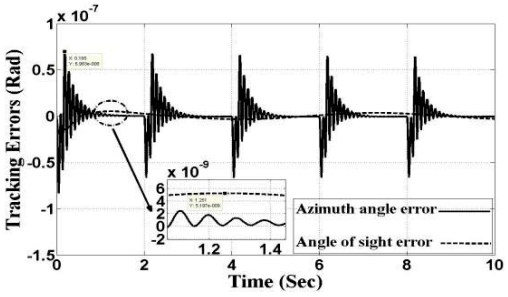

Fig. 20. Tracking errors of the joints 1 and 2, in optimal adaptive fuzzy sliding mode control, by applying disturbances are shown in Fig. 18

By comparing figures 16 and 20, it is concluded that the adaptive fuzzy sliding mode control has functioned satisfactorily and has considerably reduced the tracking error in joints 1 and 2. So that in this case, the maximum tracking error in azimuth and elevation are $6.98 \times 10^{-8}\ Rad$ and $5.2 \times 10^{-9}\ Rad$, respectively. Figure 21 shows the control inputs.

[Downloaded from jiaeee.com on 2026-09-13]
[DOR: 20.1001.1.26765810.1396.14.4.3.0]

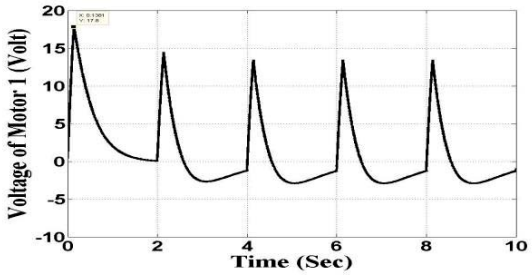

(a) Exerted control input to motor 1

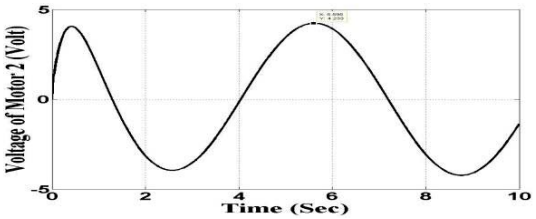

(b) Exerted control input to motor 2

Fig. 21. Exerted control inputs to motors 1 and 2, in optimal adaptive fuzzy sliding mode control, by applying disturbances are shown in Fig. 18

According to figure 21, it is clear that control inputs are free-of-chattering. On the other hand, the maximum amplitude of the input voltages of motors 1 and 2 are $17.8\,Volt$ and $4.23\,Volt$, respectively. Therefore, by comparing figure 21 with figures 17, 14, 11 and 5, we can conclude that the control inputs in this step of the simulation have the lowest amplitude and completely lack chattering. To wrap up the issues presented in section 5 of this paper and also to compare the results of the four-step simulations, four important control factors including the maximum tracking error for the joints 1 and 2, Euclidean norm of errors vector and the maximum amplitude for the control inputs as well as the chattering domain of control inputs for the proposed controllers are displayed in table 8. According to table 8, desirable performance of the proposed controller can be concluded.

Table. 8. Comparison of the simulation results

	Control Method	Maximum Tracking Errors (Rad)	Euclidean Norm of Errors Vector (Rad)	Maximum Amplitude of Control Inputs (Volt)	Chattering Domain of Control Inputs (Volt)
1	SMC	$\begin{cases} e_1 = 13.5 \times 10^{-4} \\ e_2 = 5.17 \times 10^{-5} \end{cases}$	$\|E\| = 13.51 \times 10^{-4}$	$\begin{cases} V_1 = 23.78 \\ V_2 = 6.27 \end{cases}$	$\begin{cases} V_1 \to 0.26 \ To \ 42.17 \\ V_2 \to 0.68 \ To \ 12.35 \end{cases}$
2	FSMC	$\begin{cases} e_1 = 11 \times 10^{-5} \\ e_2 = 5.1 \times 10^{-6} \end{cases}$	$\|E\| = 11.01 \times 10^{-5}$	$\begin{cases} V_1 = 19.60 \\ V_2 = 4.96 \end{cases}$	Very Negligible
3-1	AFSMC ($\varepsilon_1 = 5$ & $\varepsilon_2 = 52$)	$\begin{cases} e_1 = 11.6 \times 10^{-6} \\ e_2 = 8.90 \times 10^{-7} \end{cases}$	$\|E\| = 11.63 \times 10^{-6}$	$\begin{cases} V_1 = 18.40 \\ V_2 = 4.46 \end{cases}$	Free of Chattering
3-2	AFSMC ($\varepsilon_1 = 543$ & $\varepsilon_2 = 5420$)	$\begin{cases} e_1 = 3.47 \times 10^{-7} \\ e_2 = 3.44 \times 10^{-8} \end{cases}$	$\|E\| = 3.487 \times 10^{-7}$	$\begin{cases} V_1 = 21.50 \\ V_2 = 5.35 \end{cases}$	Free of Chattering
4	OAFSMC	$\begin{cases} e_1 = 6.98 \times 10^{-8} \\ e_2 = 5.20 \times 10^{-9} \end{cases}$	$\|E\| = 6.999 \times 10^{-8}$	$\begin{cases} V_1 = 17.80 \\ V_2 = 4.23 \end{cases}$	Free of Chattering

6. Advantages of the proposed control

In the design of the proposed control, there are some creativities and innovations which are mentioned below:

1. In the proposed control, the bounds of the existing uncertainties are decreased by accessing information of the system dynamics via the vector $\hat{u}$.
2. Using the vector $\hat{u}$ leads to the reduction of the opposite effects of the joints q_1 and q_2. Therefore, by designing two independent controllers, we can control this two-input, two-output system.
3. To estimate the bounds of the remaining uncertainties, the rule base of the adaptive fuzzy system has seven single-input, single-output fuzzy rules. Since the system has only one adaptive rule, the volume of calculations of the control input is minimal. Hence, low-speed and inexpensive processors can be used in the practical implementation of this control. On the other hand, since the vector P is determined through the adaptive fuzzy system, the bounds of the remaining uncertainties can be satisfactorily estimated and the amplitude of control input would have smooth changes; moreover, abrupt changes in the control input are prevented.
4. In most of the controllers designed for the camera stabilizer, some coefficients are considered in the controllers through which the tracking accuracy of the closed-loop system can be improved. However, this accuracy in tracking conjoins the increase in the amplitude of control input. Therefore, motors having high powers are required in the practical implementation of these controllers. In the design of the proposed control, the coefficient ε is taken into account. The increase in this coefficient can enhance the increase in tracking precision of the closed-loop system. However, an increase in this

[Downloaded from jiaeee.com on 2026-09-13]
[DOR: 20.1001.1.26765810.1396.14.4.3.0]

coefficient has a negligible effect in the increase of the amplitude of control input. This fact is demonstrated in the simulation section.

5. CSO algorithm is used in selecting the input coefficients of the proposed control. Therefore, the choice of these optimum coefficients prevents the increase in the amplitude of control input.
6. The proposed control has a small input amplitude and lacks the unfavorable phenomenon of chattering. The closed-loop system with the proposed control in the presence of uncertainties has global asymptotic stability.

7. Conclusions

In this paper, for controlling camera stabilizer a voltage-base optimal adaptive fuzzy sliding mode control was presented. At first, the known terms of dynamic equations of camera stabilizer was eliminated by utilizing inverse dynamic method. Afterwards, for the sake of overcoming the remaining uncertainties such as un-modeled dynamics and external disturbances, a voltage-base sliding mode controller was designed. Although the closed-loop system with the sliding mode control has a global asymptotic stability in the presence of the existing uncertainties, due to the use of the sgn(*) function in the control input, the occurrence of the unfavorable chattering phenomenon in the control input is unavoidable. To eliminate the unfavorable phenomenon of chattering, by using the fuzzy logic, a fuzzy sliding mode controller was proposed. Although proposed controller prevents the chattering phenomenon in the control input, choice of the coefficients of the control input should still be done using trial and error method. On the other hand, the proposed fuzzy sliding mode control lacks proof of the closed-loop system stability. In the following, to resolve the above problems, by using the fuzzy logic and concepts of the adaptive control, a voltage-base adaptive fuzzy sliding mode controller was proposed. In the proposed control, due to use of the adaptive fuzzy approximator, some of the most important coefficients of the control are updated by the adaptive rule; thereby, the possibility of chattering in the control input is eliminated. The mathematical proof reveals that closed-loop system with proposed control in the presence of structured and un-structured uncertainties, will possess global asymptotic stability. Ultimately, to access an optimum controller, other values of the control input coefficients are adjusted by the chicken swarm optimization algorithm. In the design of the optimal adaptive fuzzy sliding mode control, some points are considered which facilitates the practical implementation of this control method. Simulation results demonstrate the favorable performance of the proposed control.

References

[1] Quigley, Morgan, et al. "Target acquisition, localization, and surveillance using a fixed-wing mini-UAV and gimbaled camera." Robotics and Automation, 2005. ICRA 2005. Proceedings of the 2005 IEEE International Conference on. IEEE, (2005).

[2] A. Ghanbari Sorkhi and H. Hassanpour. " Tracking and Re-identification of People in a Network of Cameras with Disjoint Views based on Fuzzy System in Indoor Environments." Journal of Iranian Association of Electrical and Electronics Engineers 13.2 (2016): 24-41.

[3] Hurák, Zdeněk, and Martin Řezác. "Image-based pointing and tracking for inertially stabilized airborne camera platform." Control Systems Technology, IEEE Transactions on 20.5 (2012): 1146-1159.

[4] Masten MK. "Inertially stabilized platform for optical imaging systems." IEEE Control Syst Mag. 28 (2008): 47–64.

[5] Di Leo, Mario F. "System for camera stabilization." U.S. Patent No. 8,657,507. (2014).

[6] Setoodeh, Peyman, Alireza Khayatian, and Ebrahim Farjah. "Backstepping-based control of a strapdown boatboard camera stabilizer." International Journal of Control Automation and Systems 5.1 (2007): 15.

[7] Khodadadi, Hamed, Mohammad Reza Jahed Motlagh, and Mohammad Gorji. "Robust control and modeling a 2-DOF Inertial Stabilized Platform." Electrical, Control and Computer Engineering (INECCE), 2011 International Conference on. IEEE, (2011).

[8] H. Duan, S. Liu, D. Wang and X. Yu, "Design and Realization of Hybrid ACO-Based PID and luger Friction Compensation Controller for Three Degree of Freedom High Precision Flight Simulator." Simulation Modeling Practice and Theory Journal 17.6 (2009): 1160-1169.

[9] Zhou, Xiangyang, Hongyan Zhang, and Ruixia Yu. "Decoupling control for two-axis inertially stabilized platform based on an inverse system and internal model control." Mechatronics 24.8 (2014): 1203-1213.

[10] Carl Knospe, "PID Control" IEEE Control Systems Magazine 26.1 (2006): 30-32.

[11] Yonggen Han; Yanhong Lu; Haitao Qiu. "An Improved Control Scheme of Gyro Stabilization Electro-Optical Platform." Control and Automation. ICCA 2007. IEEE International Conference on. IEEE. (2007): 346-351.

[12] Abdo, MM, et al. "Stabilization loop of a two axes gimbal system using self-tuning PID type fuzzy controller." ISA transactions 53.2 (2014): 591-602.

[13] Wei Ji; Qi Li; Bo Xu; Jun-Jun Tu; De-An Zhao. "Cascade servo control for LOS stabilization of opto-electronic tracking platform design and self-tuning." Information and Automation, 2009. ICIA '09. International Conference on. IEEE. (2009): 1034-1039.

[14] S. V. Emelyanov. "Variable Structure Control Systems." Moscow: Nauka. (1967).

[15] V.I. Utkin. "Sliding mode control design principles and applications to electric drives." Industrial Electronics, IEEE Transactions on 40.1 (1993): 23-36.

[16] Smith, Brian J., et al. "Sliding mode control in a two-axis gimbal system." Aerospace Conference, 1999. Proceedings. 1999 IEEE. Vol. 5. IEEE, (1999).

[17] Tsai, Nan-Chyuan, and Bo-Yang Wu. "Nonlinear dynamics and control for single-axis gyroscope systems." Nonlinear Dynamics 51.1-2 (2008): 355-364.

[18] Hu, Yue, Yuan Cao, and Shifeng Zhang. "Design of sliding mode control with disturbance observers for

[Downloaded from jiaeee.com on 2026-09-13]

[DOR: 20.1001.1.26765810.1396.14.4.3.0]

inertial platform." Control and Decision Conference (CCDC), 2013 25th Chinese. IEEE, (2013).
[19] Shtessel, Yuri, Christopher Edwards, Leonid Fridman, and Arie Levant. "Sliding mode control and observation." Birkhäuser. (2014).
[20] Young, K. David, Vadim I. Utkin, and Umit Ozguner. "A control engineer's guide to sliding mode control." IEEE transactions on control systems technology 7.3 (1999): 328-342.
[21] Pu, Y. A. G., and L. I. Qi. "Fuzzy self-adjusting sliding mode decoupling control for gyro stabilized platform." Electric Machines and Control 5 (2008): 018.
[22] Javanfar, Elham, and Alireza Fatehi. "Modeling and fuzzy control of 3-DOF image stabilizer in presence of uncertainty and disturbance." Control System, Computing and Engineering (ICCSCE), 2011 IEEE International Conference on. IEEE, (2011).
[23] Veysi, M, and Soltanpour, MR. "Eliminating chattering phenomenon in sliding mode control of robot manipulators in the joint space using fuzzy logic." Journal of Solid and Fluid Mechanic 2.3 (2012): 45-54.
[24] Veysi, M. "A New Robust Fuzzy Sliding Mode Control of Robot manipulator in the Task Space in Presence of Uncertainties." International Journal of Scientific & Engineering Research 6.6 (2015): 372-381.
[25] Yau, Her-Terng, and Chieh-Li Chen. "Chattering-free fuzzy sliding-mode control strategy for uncertain chaotic systems." Chaos, Solitons & Fractals 30.3 (2006): 709-718.
[26] Chen, Chieh-Li, and Ming-Hui Chang. "Optimal design of fuzzy sliding-mode control: a comparative study." Fuzzy Sets and Systems 93.1 (1998): 37-48.
[27] Stengel, Robert F. "Optimal control and estimation." Courier Corporation, (2012).
[28] Soltanpour, MR, and Khooban, MH. "A particle swarm optimization approach for fuzzy sliding mode control for tracking the robot manipulator." Nonlinear Dynamics 74.1–2 (2013): 467–478.
[29] Veysi, M, Soltanpour, MR, and Khooban, MH. "A novel self-adaptive modified bat fuzzy sliding mode control of robot manipulator in presence of uncertainties in task space." Robotica (2014): 1-20.
[30] Soltanpour MR, Khooban MH, and Khalghani MR. "An optimal and intelligent control strategy for a class of nonlinear systems: adaptive fuzzy sliding mode." Journal of Vibration and Control (2014): 1077546314526920.
[31] Khazaee, Mostafa, Amir HD Markazi, and Ehsan Omidi. "Adaptive fuzzy predictive sliding control of uncertain nonlinear systems with bound-known input delay." ISA Transactions (2015).
[32] Yoshimura, Toshio. "Adaptive fuzzy sliding mode control for uncertain multi-input multi-output discrete-time systems using a set of noisy measurements." International Journal of Systems Science 46.2 (2015): 255-270.
[33] Benbrahim M, Essounbouli N, Hamzaoui A and Betta A. "Adaptive type-2 fuzzy sliding mode controller for SISO nonlinear systems subject to actuator faults." International Journal of Automation and Computing 10.4 (2013): 335–342.
[34] Han H (2011) "Adaptive fuzzy sliding-mode control for a class of nonlinear systems with uncertainties." In: 2011 IEEE International Conference on Fuzzy Systems (FUZZ), Taipei, (2011): 1320–1326.
[35] Essounbouli N and Hamzaoui A. "Direct and indirect robust adaptive fuzzy controllers for a class of nonlinear systems." International Journal of Control Automation and Systems 4.2 (2006): 146-154.
[36] Wang J, Peng H, Chen YY and Song ZQ. "Adaptive fuzzy wavelet control for a class of uncertain nonlinear systems." In: International Conference on Machine Learning and Cybernetics, (2006): 288–292.
[37] Sharkawy AB and Salman SA. "An adaptive fuzzy sliding mode control scheme for robotic systems." Intell. Control and Automation 2.4 (2011): 299–309.
[38] Fateh, MM. "Robust control of flexible-joint robots using voltage control strategy." Nonlinear Dynamics 67.2 (2012): 1525–1537.
[39] Veysi, M, and Soltanpour, MR. "Voltage-Base Control of Robot Manipulator Using Adaptive Fuzzy Sliding Mode Control." International Journal of Fuzzy Systems 19.5 (2017): 1430-1443.
[40] J. Faiz and A. R. Ghaffari. "Adaptive Position Control of Permanent Magnet Synchronous Motor Drives using Neural Networks." Journal of Iranian Association of Electrical and Electronics Engineers 1.2 (2004): 21–26.
[41] M. W. Spong and M. Vidyasagar, "Robot Dynamics and Control." John Wiley and Sons, Inc, (1989).
[42] J. J. E. Slotine and W. Li. "Applied Nonlinear Control." Prentice-Hall (1991).
[43] Wang LX. "A Course in Fuzzy Systems." New Jersey: Prentice-Hall Press, (1997).
[44] Meng, Xianbing, et al. "A new bio-inspired algorithm: chicken swarm optimization." Advances in swarm intelligence. Springer International Publishing, (2014): 86-94.

[Downloaded from jiaeee.com on 2026-09-13]
[DOR: 20.1001.1.26765810.1396.14.4.3.0]